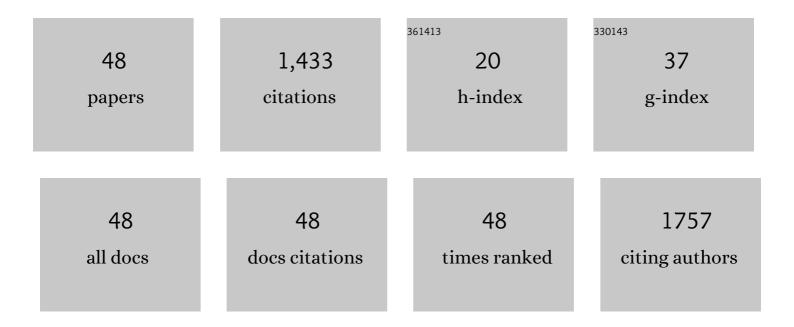
Ji-min yang

List of Publications by Year in descending order

Source: https://exaly.com/author-pdf/1969078/publications.pdf Version: 2024-02-01



ILMIN VANC

#	Article	IF	CITATIONS
1	Adsorptive removal of organic dyes from aqueous solution by a Zr-based metal–organic framework: effects of Ce(<scp>iii</scp>) doping. Dalton Transactions, 2018, 47, 3913-3920.	3.3	161
2	A facile approach to fabricate an immobilized-phosphate zirconium-based metal-organic framework composite (UiO-66-P) and its activity in the adsorption and separation of organic dyes. Journal of Colloid and Interface Science, 2017, 505, 178-185.	9.4	88
3	Fabrication of a carbon quantum dots-immobilized zirconium-based metal-organic framework composite fluorescence sensor for highly sensitive detection of 4-nitrophenol. Microporous and Mesoporous Materials, 2019, 274, 149-154.	4.4	84
4	Cucurbit[6]uril-Based Supramolecular Assemblies: Possible Application in Radioactive Cesium Cation Capture. Journal of the American Chemical Society, 2014, 136, 16744-16747.	13.7	82
5	Shape and size control and gas adsorption of Ni(II)-doped MOF-5 nano/microcrystals. Microporous and Mesoporous Materials, 2014, 190, 26-31.	4.4	77
6	Facile water-stability evaluation of metal–organic frameworks and the property of selective removal of dyes from aqueous solution. Dalton Transactions, 2016, 45, 8753-8759.	3.3	76
7	Effect of the Synergetic Interplay between the Electrostatic Interactions, Size of the Dye Molecules, and Adsorption Sites of MIL-101(Cr) on the Adsorption of Organic Dyes from Aqueous Solutions. Crystal Growth and Design, 2018, 18, 7533-7540.	3.0	62
8	High-performance electrochemical sensing of circulating tumor DNA in peripheral blood based on poly-xanthurenic acid functionalized MoS 2 nanosheets. Biosensors and Bioelectronics, 2018, 105, 116-120.	10.1	61
9	Rapid adsorptive removal of cationic and anionic dyes from aqueous solution by a Ce(III)-doped Zr-based metal–organic framework. Microporous and Mesoporous Materials, 2020, 292, 109764.	4.4	56
10	Controlled Synthesis of Porous Coordinationâ€Polymer Microcrystals with Definite Morphologies and Sizes under Mild Conditions. Chemistry - A European Journal, 2014, 20, 14783-14789.	3.3	53
11	Co(II)-doped MOF-5 nano/microcrystals: Solvatochromic behaviour, sensing solvent molecules and gas sorption property. Journal of Solid State Chemistry, 2014, 218, 50-55.	2.9	47
12	Effect of Synergistic Interplay between Surface Charge, Crystalline Defects, and Pore Volume of MIL-100(Fe) on Adsorption of Aqueous Organic Dyes. Industrial & Engineering Chemistry Research, 2020, 59, 2113-2122.	3.7	44
13	Metal ion induced porous HKUST-1 nano/microcrystals with controllable morphology and size. CrystEngComm, 2016, 18, 4127-4132.	2.6	40
14	Effect of surface charge status of amorphous porous coordination polymer particles on the adsorption of organic dyes from an aqueous solution. Journal of Colloid and Interface Science, 2018, 525, 54-61.	9.4	40
15	Effect of free carboxylic acid groups in UiO-66 analogues on the adsorption of dyes from water: Plausible mechanisms for adsorption and gate-opening behavior. Journal of Molecular Liquids, 2019, 283, 160-166.	4.9	38
16	Superior selective adsorption of anionic organic dyes by MIL-101 analogs: Regulation of adsorption driving forces by free amino groups in pore channels. Journal of Molecular Liquids, 2020, 302, 112616.	4.9	32
17	Modulation of the driving forces for adsorption on MIL-101 analogues by decoration with sulfonic acid functional groups: superior selective adsorption of hazardous anionic dyes. Dalton Transactions, 2020, 49, 6651-6660.	3.3	29
18	Controlled growth and gas sorption properties of IRMOF-3 nano/microcrystals. Dalton Transactions, 2014, 43, 16707-16712.	3.3	26

JI-MIN YANG

#	Article	IF	CITATIONS
19	Shape-controlled synthesis and photocatalytic activity of In 2 O 3 nanostructures derived from coordination polymer precursors. Chinese Chemical Letters, 2016, 27, 492-496.	9.0	26
20	Facile fabrication of MIL-103(Eu) porous coordination polymer nanostructures and their sorption and sensing properties. Dalton Transactions, 2016, 45, 5841-5847.	3.3	26
21	Superior adsorptive removal of azo dyes from aqueous solution by a Ni(II)-doped metal–organic framework. Colloids and Surfaces A: Physicochemical and Engineering Aspects, 2021, 619, 126549.	4.7	19
22	A facile approach to fabricate porous UMCM-150 nanostructures and their adsorption behavior for methylene blue from aqueous solution. CrystEngComm, 2015, 17, 4825-4831.	2.6	17
23	Functionally modified metal–organic frameworks for the removal of toxic dyes from wastewater. CrystEngComm, 2022, 24, 434-449.	2.6	17
24	Effect of additives on morphology and size and gas adsorption ofÂSUMOF-3 microcrystals. Microporous and Mesoporous Materials, 2016, 222, 27-32.	4.4	15
25	Superior adsorptive removal of anionic dyes by MIL-101 analogues: the effect of free carboxylic acid groups in the pore channels. CrystEngComm, 2019, 21, 5824-5833.	2.6	15
26	Modulation of driving forces fo UiO-66 analog adsorbents by decoration with amino functional groups: Superior adsorption of hazardous dyes. Journal of Molecular Structure, 2020, 1220, 128716.	3.6	15
27	Porous ZnO and ZnO–NiO composite nano/microspheres: synthesis, catalytic and biosensor properties. RSC Advances, 2014, 4, 51098-51104.	3.6	14
28	MOF-derived hollow NiO–ZnO composite micropolyhedra and their application in catalytic thermal decomposition of ammonium perchlorate. Russian Journal of Physical Chemistry A, 2017, 91, 1214-1220.	0.6	13
29	Construction of self-signal DNA electrochemical biosensor employing WS ₂ nanosheets combined with PIn6COOH. RSC Advances, 2019, 9, 9613-9619.	3.6	13
30	Surface-Functionalized MoS ₂ Nanosheets Sensor for Direct Electrochemical Detection of PIK3CA Gene Related to Lung Cancer. Journal of the Electrochemical Society, 2020, 167, 027501.	2.9	13
31	Morphology evolution and gas adsorption of porous metal–organic framework microcrystals. Dalton Transactions, 2015, 44, 16888-16893.	3.3	12
32	Solubility in the ternary system LiCl + MgCl2 + H2O at 60 and 75°C. Russian Journal of Physical Chemistry A, 2010, 84, 1169-1173.	0.6	11
33	Solubilities of salts in the ternary systems NaCl + CaCl2 + H2O and KCl + CaCl2 + H2O at 75°C. Russian Journal of Physical Chemistry A, 2011, 85, 1149-1154.	0.6	11
34	Measurement of Solubilities in the Ternary System NaCl + CaCl2+ H2O and KCl + CaCl2+ H2O at 50℃. Journal of the Korean Chemical Society, 2010, 54, 269-274.	0.2	11
35	Isopiestic Determination of the Osmotic Coefficients andÂPitzer Model Representation forÂtheÂLi2B4O7+LiCl + H2O System at T=298.15ÂK. Journal of Solution Chemistry, 2008, 37, 377-389.	1.2	10
36	Effect of particle size distribution of UiO-67 nano/microcrystals on the adsorption of organic dyes from aqueous solution. CrystEngComm, 2018, 20, 5672-5676.	2.6	10

JI-MIN YANG

#	Article	IF	CITATIONS
37	Electrochemical determination of PIK3CA gene associated with breast cancer based on molybdenum disulfide nanosheet-supported poly(indole-6-carboxylic acid). Analytical Methods, 2019, 11, 157-162.	2.7	10
38	Tungsten disulfide nanosheets supported poly(xanthurenic acid) as a signal transduction interface for electrochemical genosensing applications. RSC Advances, 2018, 8, 39703-39709.	3.6	9
39	Sulfo-modified MIL-101 with immobilized carbon quantum dots as a fluorescence sensing platform for highly sensitive detection of DNP. Inorganica Chimica Acta, 2021, 519, 120276.	2.4	9
40	Highly Sensitive and Selective Detection of 2,4-Dinitrophenol by a Fluorescent Amine-Functionalized Carbon Quantum Dot@Metal-Organic Framework. Russian Journal of Physical Chemistry A, 2019, 93, 2452-2457.	0.6	7
41	Self-Signal Electrochemical Monitoring of Hybridization of Nucleic Acids Based on Riboflavine Sodium Phosphate Decorated WS ₂ Nanosheets. Journal of the Electrochemical Society, 2020, 167, 027502.	2.9	7
42	MIL-100(Fe)@GO composites with superior adsorptive removal of cationic and anionic dyes from aqueous solutions. Journal of Molecular Structure, 2022, 1265, 133365.	3.6	7
43	The phase diagrams and Pitzer model representations for the system KCl + MgCl2 + H2O at 50 and 75°C. Russian Journal of Physical Chemistry A, 2012, 86, 1930-1935.	0.6	6
44	Osmotic Coefficients of the Li2B4O7+LiCl + H2O System at T=273.15 K. Journal of Solution Chemistry, 2009, 38, 429-439.	1.2	4
45	Solid-liquid phase equilibria at 50 and 75°C in the NaCl + MgCl2 + H2O system and the pitzer model representations. Russian Journal of Physical Chemistry A, 2013, 87, 2195-2199.	0.6	4
46	The phase equilibriums in the NH4Cl-CaCl2-H2O system at 50 and 75°C and their Pitzer model representations. Russian Journal of Physical Chemistry A, 2014, 88, 2325-2330.	0.6	4
47	Controlled growth and DNA sensing property of HKUST-1@GrO nanocomposites. Materials Letters, 2017, 209, 142-145.	2.6	2
48	Electrochemical self-signal switch for determination of KRAS gene employingÂriboflavin 5'-adenosine diphosphate functionalized MoS2 nanosheets. Journal of Solid State Electrochemistry, 0, , 1.	2.5	0